

Dynamic Recrystallization Models of AerMet100 Ultrahigh-strength Steel During Thermo-mechanical Processing

Zhao Zhanglong, Min Xiaonan, Xu Wenxin, Cao Lanchuan, Zhang Ge, Song Xu-yang, Li Hui

Northwestern Polytechnical University, Xi'an 710072, China

Abstract: In order to accurately predict the microstructure evolution during thermo-mechanical processing of AerMet100 ultrahigh-strength steel, the dynamic recrystallization (DRX) models including DRX volume fraction and DRX grain size were established by conducting a series of isothermal hot compression tests. The hot deformation behavior of the alloy in a wide range of temperatures from 800 °C to 1040 °C, strain rates from 0.01 s⁻¹ to 10 s⁻¹ and deformation degree from 15% to 60% was analyzed. The Zener-Hollomon parameter of the constitutive model for the AerMet100 steel was obtained to establish DRX models. The effects of deformation parameters on the microstructural evolution were quantitatively predicted through the established DRX models. The microstructure observation shows that higher temperature, lower strain rate and larger deformation degree are beneficial to the homogenization and refinement of the microstructure due to the occurrence of DRX. The good agreement between the prediction and the experiment validates the accuracy of the established DRX models, indicating that the DRX models can be used to quantitatively predict the microstructure evolution of AerMet100 steel components during thermo-mechanical processing under different hot deformation conditions.

Key words: AerMet100 steel; dynamic recrystallization; hot deformation; microstructure

AerMet100 ultrahigh-strength steel is extensively applied in the rocket engine casings, bulletproof steel plates and landing gear in aerospace industry. The alloy displays high strength, ductility, fracture toughness, fatigue resistance and excellent stress corrosion cracking resistance^[1-4]. The further thermo-mechanical processing of hot rolled AerMet100 steel bar is usually conducted above the recrystallization temperature to obtain the complex shape and the mechanical properties of components. During thermo-mechanical processing, the microstructural morphology and mechanical properties of AerMet100 steel can be effectively improved under appropriate hot deformation conditions due to the work hardening (WH), and dynamic recovery (DRV) and dynamic recrystallization (DRX) can affect the microstructural transformation. Compared to WH and DRV, DRX plays an important role in improving the microstructure refinement for the low stacking

fault energy of AerMet100 steel. Therefore, it is of great significance to predict the DRX behavior of the alloy under different deformation conditions and to quantitatively characterize the relationship between the microstructure and deformation parameters.

In order to accurately control the microstructure and mechanical properties of the components, some studies have been investigated on the hot deformation behavior of AerMet100 steel. Ji et al^[5-7] described the hot deformation behavior of AerMet100 steel in the temperature ranges of 800~1200 °C and strain rate ranges of 0.01~50 s⁻¹ using the Arrhenius constitutive model and artificial neural network (ANN) constitutive model. And the optimum hot processing windows at temperatures of 1025~1200 °C and strain rates of 0.03~15 s⁻¹ were determined by establishing the hot processing maps. Furthermore, the models of DRX fraction and grain size

Received date: February 20, 2020

Foundation item: National Natural Science Foundation of China (51974259); Natural Science Foundation of Shannxi Province (2019JM005)

Corresponding author: Zhao Zhanglong, Ph. D., Associate Professor, School of Materials Science and Engineering, Northwestern Polytechnical University, Xi'an 710072, P. R. China, Tel: 0086-29-88492642, E-mail: zljzhao@nwpu.edu.cn

Copyright © 2020, Northwest Institute for Nonferrous Metal Research. Published by Science Press. All rights reserved.

were established by the analysis of peak stress and critical stress from flow stress-strain curves of hot compression test. And the results indicate that the DRX grain size is only dependent on Zener-Hollomon parameter. Hu et al^[8,9] pointed out that AerMet100 steel is strongly sensitive to the strain rate based on the quasi-static and dynamic tests at different strain rates. These previous references provide a detailed description for understanding the hot deformation behavior of AerMet100 steel. Since the DRX plays an important role in the microstructure evolution, the DRX behavior of Aermet100 steel during hot deformation has been studied. However, the models of DRX fraction and DRX grain size of AerMet100 steel from the experimental analysis are insufficient for meeting the actual thermos-mechanical processing requirements.

In the present work, the isothermal compression tests under different deformation conditions were conducted to investigate the deformation behavior and microstructure evolution of AerMet100 ultrahigh-strength steel during thermo-mechanical processing. The models including DRX fraction and DRX grain size were established based on the microstructural observation. The effects of deformation parameters on the DRX fraction and grain size were predicted according to the established DRX models. The comparison between the predicted and experimental results indicates that the proposed models can be used to quantitatively predict the microstructure evolution of AerMet100 ultrahigh-strength steel during thermo-mechanical processing.

1 Experiment

The material used in this investigation was AerMet100 ultrahigh-strength steel, and the chemical composition of the alloy is shown in Table 1. The initial microstructure with the average grain size of approximate 30 μm is shown in Fig.1. To investigate the deformation behavior of the alloy, cylindrical specimens with a diameter of 10 mm and a height of 15 mm (Fig.2) were machined for isothermal compression tests. The isothermal compression tests were carried out on a Gleeble-3500 thermo-mechanical simulator at temperatures of 800~1040 $^{\circ}\text{C}$, strain rates of 0.01~10 s^{-1} and height reductions of 15%~60%. During the tests, the specimen was heated to the deformation temperature with a constant heating rate of 10 $^{\circ}\text{C/s}$, soaked for 5 min, and then compressed to the desired height reduction at a constant strain rate. The thermocouple was welded in the center of the specimen to monitor and record the variation of actual temperature. The data during compression tests under different deformation conditions were automatically recorded and converted to the true stress-true strain data. The specimens were water quenched immediately upon the completion of compression to preserve the microstructure at elevated temperatures. Some typical compressed specimens were sectioned parallel to the compression direction for metallographic examination through an OLYMPUS-GX71 optical microscope (OM).

Table 1 Chemical composition of Aermet100 ultrahigh-strength steel (wt%)

Ni	Co	Cr	Mo	C	Ti	Mn	Si	Fe
11.3	13.45	3.04	1.26	0.22	0.015	0.10	0.10	Bal.

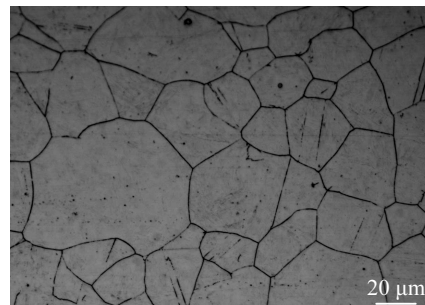


Fig.1 Initial microstructure of AerMet100 steel

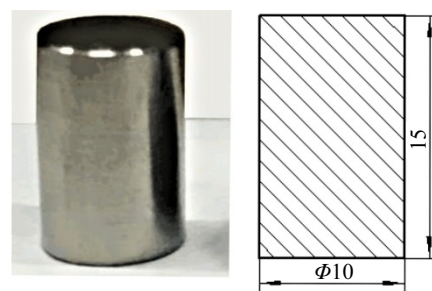


Fig.2 Schematic diagram of the cylindrical specimens

2 Results and Discussion

2.1 Analysis of flow behavior

The typical true stress-true strain curves of AerMet100 ultrahigh-strength steel isothermally compressed at different temperatures and strain rates are shown in Fig.3. It can be observed that the flow stress firstly increases rapidly to the peak value and then gradually decreases to a steady state with the increase of strain, which is a comprehensive reflection of WH, DRV and DRX. At the early stage of deformation, the formation and proliferation of the dislocation result in the work hardening. And the softening of DRV caused by dislocation climbing, slipping or cross slipping is not enough to counteract the effects of WH, leading to the stress increase to a critical value. Then the DRX grains start to nucleate and grow under the critical stress, and the increase of dislocation density due to the predominance of WH can continuously promote the nucleation of DRX grains^[10]. Therefore, the flow stress gradually increases to a peak value at a moment of achieving the instantaneous equivalence between the hardening rate and softening rate. As the AerMet100 steel is a kind of low stacking fault energy metal, the DRX is the main restoration mechanism during the hot deformation which can

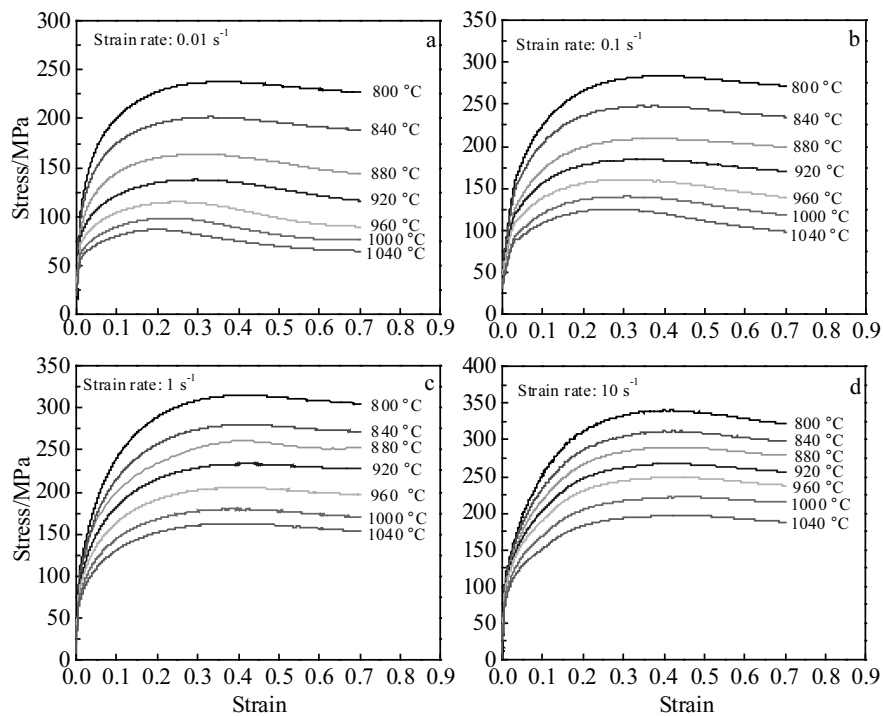


Fig.3 Typical true stress-strain curves of AerMet100 steel at different deformation temperatures and strain rates: (a) 0.01 s^{-1} , (b) 0.1 s^{-1} , (c) 1 s^{-1} , and (d) 10 s^{-1}

weaken the effect of WH on the variation of flow stress and slightly declines the flow stress after the peak value^[11]. Finally, the flow steady state appears permanently when a new balance between softening rate and hardening rate is achieved.

The flow stress changes obviously with strain rate and temperature, which reveals the strong sensitivity of flow behavior to deformation conditions. The peak stress values under different deformation conditions are plotted in Fig.4 to analyze the relationship between flow stress and deformation parameters.

Evidently, the peak flow stress gradually decreases with the increase of deformation temperature and the decrease of strain

rate since the dislocation annihilation rate becomes faster at higher deformation temperature, resulting in a part of decline of flow stress. In contrast, when the alloy is deformed at higher strain rate, the dislocation multiplication rate is faster which may intensify the influence of WH. And the nucleation and growth of DRX grains are promoted at higher deformation temperature and lower strain rate^[12]. This can be ascribed to the higher temperature which greatly promotes the grain boundary mobility and increases the thermal activation energy. The lower strain rate can provide enough deformation time to accumulate energy for the nucleation of DRX grains^[13-16].

2.2 Constitutive model

The Arrhenius type equations are used to establish the constitutive model for AerMet100 steel and designated as follows^[17]:

$$\dot{\epsilon} = \begin{cases} A_1 \sigma^{n_1} \exp(-Q/RT) & \text{when } \alpha\sigma < 0.8 \\ A_2 \exp(\beta\sigma) \exp(-Q/RT) & \text{when } \alpha\sigma > 0.8 \\ A[\sinh(\alpha\sigma)]^n \exp(-Q/RT) & \text{for all values of } \alpha\sigma \end{cases} \quad (1)$$

where A_1 , A_2 , A , and α are material constants; n_1 , n and β are the parameters related to strain rate sensitivity; R is gas constant; T is absolute temperature (K); Q is deformation activation energy (J/mol); $\dot{\epsilon}$ is strain rate; σ is the flow stress.

In this study, the hyperbolic sine equation is adopted to establish the relationship between deformation parameters and flow stress of AerMet100 steel. The values of the material constant in Eq.(1) can be obtained based on the stress-strain

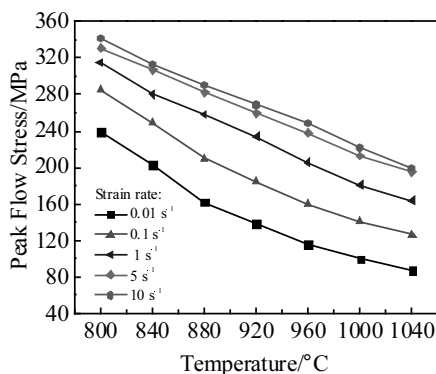


Fig.4 Peak stress of the AerMet100 steel compressed under different conditions

date from hot compression tests. According to regression analysis, the material constants can be obtained by substituting the values of peak flow stress and corresponding strain rate into Eq.(1). As indicated in Fig.5, the values of β and n_1 can be obtained from the slope of linear fitting of the plot of $\sigma - \ln \dot{\epsilon}$ and $\ln \sigma - \ln \dot{\epsilon}$, respectively. Then the value of α under the peak stress is calculated to be 0.00518 MPa^{-1} .

The value of n can be calculated from the linear fitting of the plot of $\ln[\sinh(\alpha\sigma)] - \ln \dot{\epsilon}$, as shown in Fig.6a, which is the reciprocals of the average slopes of the lines at all temperatures. The value of n in the present deformation conditions is 8.109. Deformation activation energy Q is used to measure the difficulty of rearrangement of atoms in the process of thermo-mechanical deformation, which is affected by material characteristics and deformation conditions. Assuming that the deformation activation energy Q does not change with deformation temperature, the equation of deformation activation energy Q can be calculated by:

$$Q = R \frac{\partial[\ln(\sinh(\alpha\sigma))]}{\partial(1/T)} \bigg/ \frac{\partial[\ln(\sinh(\alpha\sigma))]}{\partial(\ln \dot{\epsilon})} \quad (2)$$

And the value of Q can be obtained from the plots shown in Fig.6, which is the quotient of the average slopes of two groups of lines above. The value of Q can be calculated to be 396.724 kJ/mol based on the peak flow stress. This deformation activation energy value is in agreement with the results in previous researches on AerMet100 steel^[6]. The temperature compensated strain rate parameter, also known as the Zener-Hollomon parameter^[18,19], is defined as:

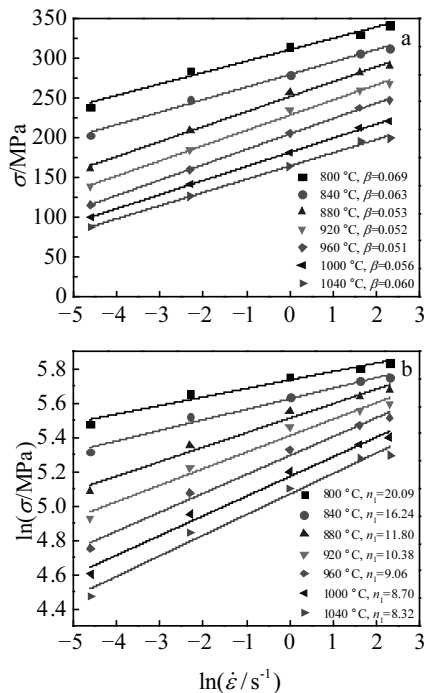


Fig.5 Plot of $\sigma - \ln \dot{\epsilon}$ (a) and $\ln \sigma - \ln \dot{\epsilon}$ (b)

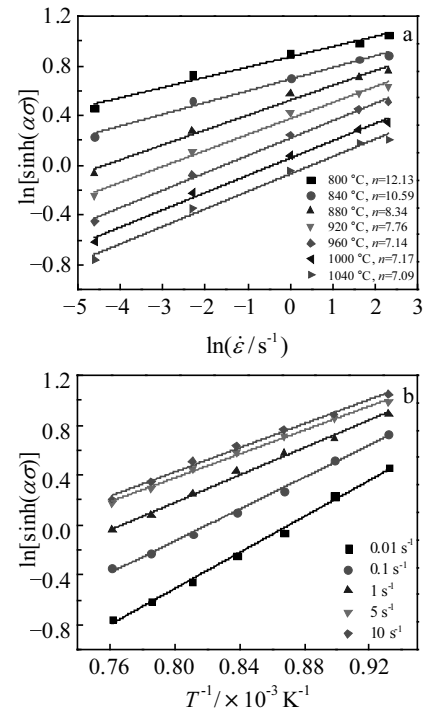


Fig.6 Plot of $\ln[\sinh(\alpha\sigma)]$ vs $\ln \dot{\epsilon}$ (a) and $\ln[\sinh(\alpha\sigma)]$ vs T^{-1} (b)

$$Z = \dot{\epsilon} \exp(Q/RT) = A [\sinh(\alpha\sigma)]^n \quad (3)$$

The parameter A can be obtained according to the relationship between $\ln Z$ and $\ln[\sinh(\alpha\sigma)]$ at different temperatures and strain rates. Based on the plot in Fig.7, the calculated value of $\ln A$ is 37.07. Therefore, the constitutive model of AerMet100 steel can be obtained, which is described as:

$$\dot{\epsilon} = e^{37.07} [\sinh(5.18 \times 10^{-3} \sigma)]^{8.109} \exp(-396724/RT) \quad (4)$$

In order to verify accuracy of proposed constitutive model, the correlation coefficient (R) and average absolute relative error (AARE) are characterized, which can be expressed as:

$$R = \frac{\sum_{i=1}^N (E_i - \bar{E})(P_i - \bar{P})}{\sqrt{\sum_{i=1}^N (E_i - \bar{E})^2 \sum_{i=1}^N (P_i - \bar{P})^2}} \quad (5)$$

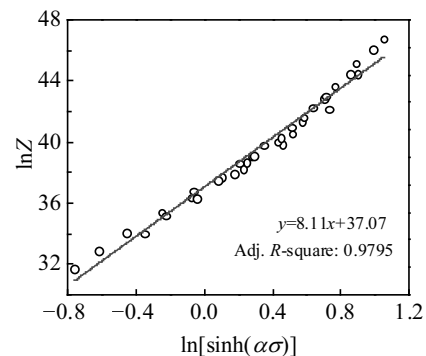


Fig.7 Plot of $\ln Z$ vs $\ln[\sinh(\alpha\sigma)]$

$$\text{AARE} = \frac{1}{N} \sum_{i=1}^N \left| \frac{E_i - P_i}{E_i} \right| \times 100\% \quad (6)$$

where E_i denotes the experimental stress and P_i denotes the calculated flow stress. \bar{E} and \bar{P} are the mean values. N is the total number of the data points used for comparison. The coefficient (R) and average absolute relative error (AARE) between all the calculated and selected experimental data are 0.9798 and 4.31%, respectively. The experimental and predicted values of peak stress are plotted as scatter plots and compared to the best fitting line, as shown in Fig.8. As shown in the figure, most of the data points stay fairly close to the best regression line and the predicted results of peak flow stresses are in good agreement with the experimental results. The results indicate that the established model is capable for predicting the flow stress of AerMet100 steel during hot deformation.

2.3 Microstructure analysis

The microstructures of AerMet100 steel compressed under different deformation conditions are shown in Fig.9~11. Fig.9 illustrates the effect of temperature on the microstructure of the steel. At the low temperature of 880 °C, the original microstructure is transformed to dynamic recrystallized microstructure and the smaller DRX grains are predominantly distributed in original grain boundaries, as shown in Fig.9a. It is obvious that the fraction and grain size of DRX increase with increasing the temperature. This may be ascribed to the faster rate of thermally activated processes for DRX grain nucleation and growth at higher temperatures. And the grain

boundary mobility (growth kinetics) or the sliding and rearrangement of dislocations become more remarkable at higher deformation temperatures^[20-22].

The effects of strain rate on the microstructures of AerMet100 steel are listed in Fig.10. As shown in Fig.10, both the DRX volume fraction and DRX grain size decrease with the increase of strain rate. It can be seen that the fine and homogeneous DRX grains are distributed within the original grains and grain boundaries at a lower strain rate of 0.01 s⁻¹. With increasing the strain rate to 10 s⁻¹, a few small DRX grains are distributed in the original grain boundaries. The extent of DRX is insufficient and a small number of residual deformation microstructures can be observed. At relatively higher strain rate, the diffusion for nucleation is restrained and the deformation time is not enough for the growth of DRX grain^[23].

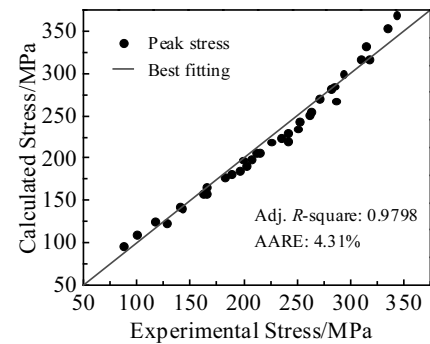


Fig.8 Linear relationship of experimental and predicted peak stress

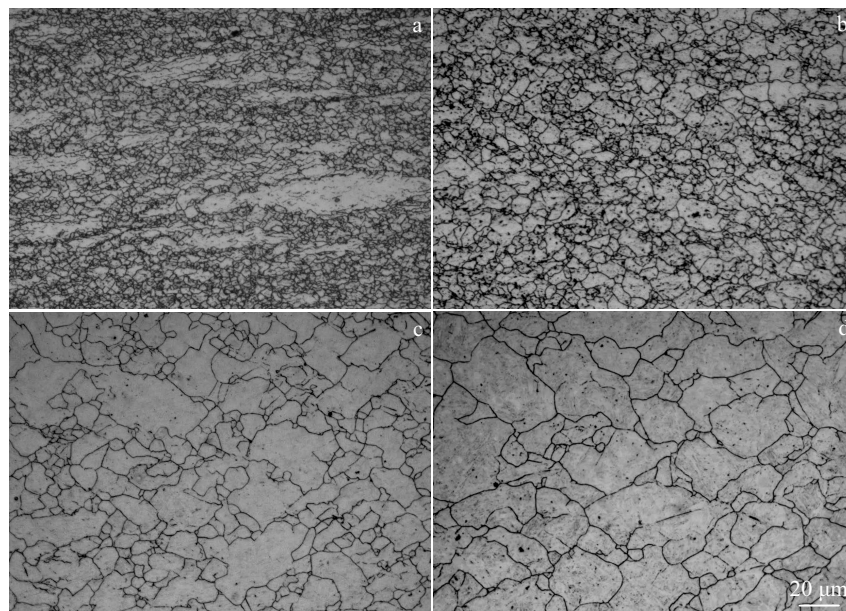


Fig.9 Microstructures of AerMet100 steel at a strain rate of 0.01 s⁻¹ and a height reduction of 60% at different temperatures: (a) 880 °C, (b) 920 °C, (c) 1000 °C, and (d) 1040 °C

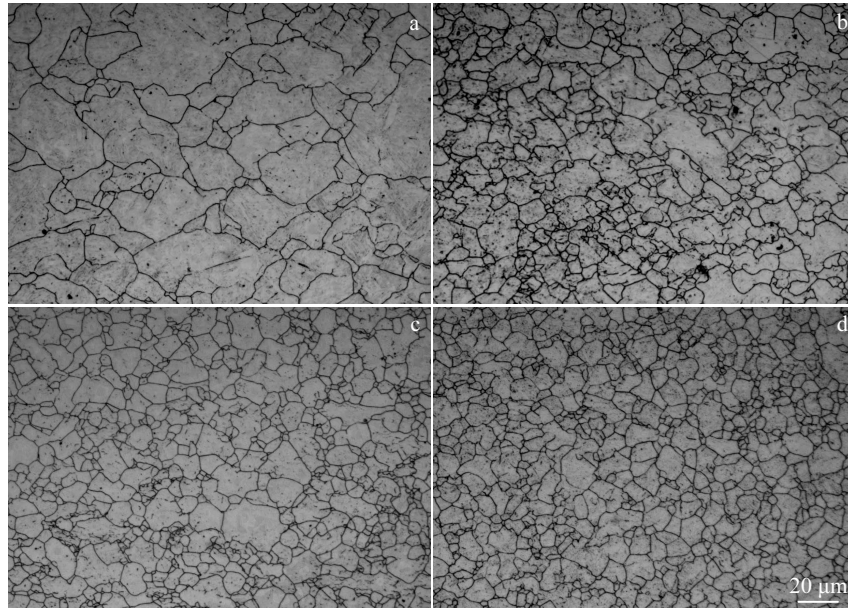


Fig.10 Microstructures of AerMet100 steel at a temperature of 1040 °C and a height reduction of 60% with different strain rates: (a) 0.01 s^{-1} , (b) 0.1 s^{-1} , (c) 1 s^{-1} , and (d) 10 s^{-1}

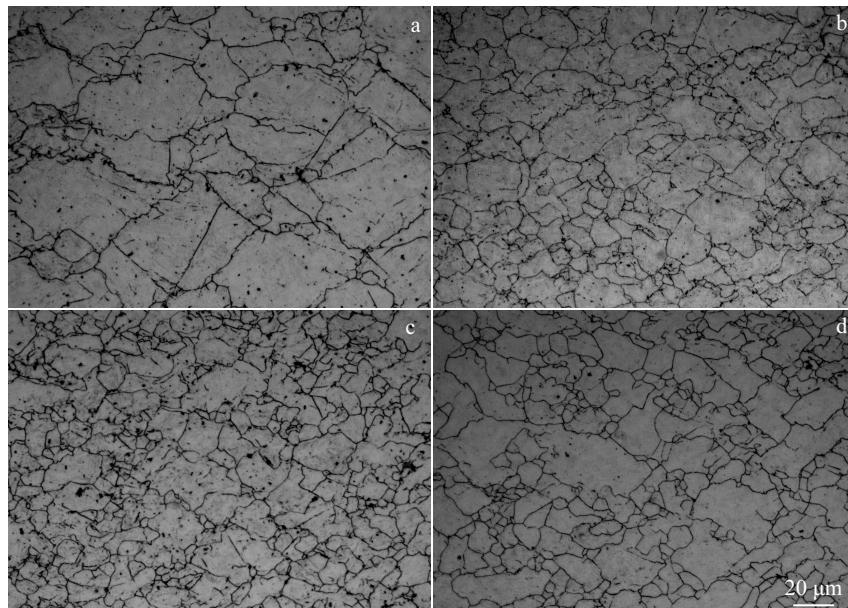


Fig.11 Microstructures of AerMet100 steel at a temperature of 1000 °C and a strain rate of 0.01 s^{-1} with different height reductions: (a) 15%, (b) 30%, (c) 45%, and (d) 60%

Fig.11 illustrates the effects of strain on the microstructures of AerMet100 steel. When the height reduction increases from 15% to 60%, the DRX fraction reaches over 90%, and the finer grain size and more uniform microstructure are obtained, as shown in Fig.11. This is because the deformation storage energy increases with the increase of deformation degree,

which can promote the nucleation and growth of recrystallized grains. At the height reduction of 15%~30% shown in Fig.11b and 11d, the strain is not enough to produce complete DRX. According to above analysis, the complete DRX can be achieved under the conditions of high temperature, low strain rate and large deformation.

2.4 Model for DRX volume fraction

The occurrence of DRX under different deformation conditions can be proved according to the microstructure observation. In order to accurately predict DRX behaviors during the hot forging process, it is significant to establish the DRX models. The Avrami relation^[24] is a general approach to describe the transformation of one phase to another under certain conditions, which can be applied to characterize the DRX behavior of AerMet100 steel. It can be expressed as:

$$X_{\text{DRX}} = 1 - \exp \left(-0.693 \left(\frac{t}{t_{0.5}} \right)^p \right) \quad (7)$$

where X_{DRX} is the DRX volume fraction; $t_{0.5}$ is the time when the volume fraction of DRX is 50%; t is deformation time, p is the Avrami constant. The following DRX volume fraction relationship can be deduced from Eq.(7):

$$X_{\text{DRX}} = 1 - \exp \left(-0.693 \left(\frac{\varepsilon}{\varepsilon_{0.5}} \right)^p \right) \quad (8)$$

where $\varepsilon_{0.5}$ is the strain for the 50% complete DRX. The DRX volume fraction is determined based on the microstructure measurements under different deformation conditions. The previous works^[25,26] proposed the relationship between $\varepsilon_{0.5}$ and the parameter Z , which is expressed as $\varepsilon_{0.5} = BZ^q$. The values of Z under different deformation conditions have been obtained in Section 2.2. The parameter values of B and q can be obtained from the linear fitting of the plot of $\ln Z - \ln \varepsilon_{0.5}$, as shown in Fig.12. The calculated values of B and q are 0.359 and 0.0655, respectively.

Using the same method, the value of parameter p can be deduced from the linear fitting of the plot of $\ln[-\ln(1 - X_{\text{DRX}})] - \ln(\varepsilon/\varepsilon_{0.5})$, as shown in Fig.13. The value of p can be obtained as 2.532. Hence, the model of DRX volume fraction for the AerMet100 steel can be described as:

$$\begin{cases} X_{\text{DRX}} = 1 - \exp \left(-0.693 \left(\frac{\varepsilon}{\varepsilon_{0.5}} \right)^{2.532} \right) \\ \varepsilon_{0.5} = 0.359 Z^{0.0655} \end{cases} \quad (9)$$

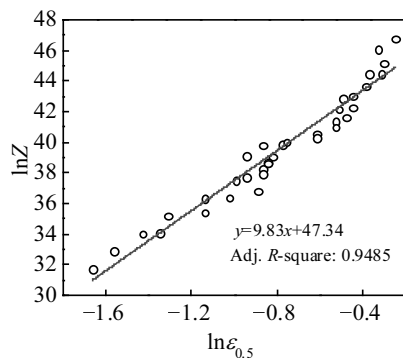


Fig.12 Plot of $\ln Z$ vs $\ln \varepsilon_{0.5}$

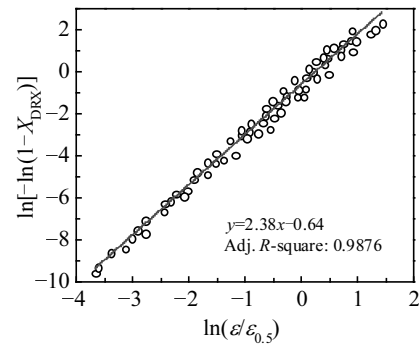


Fig.13 Plot of $\ln[-\ln(1 - X_{\text{DRX}})]$ vs $\ln(\varepsilon/\varepsilon_{0.5})$

According to the established DRX models, the DRX volume fraction under different deformation conditions can be calculated. The comparison between the calculated (solid line) and experimental (symbol) DRX volume fraction in the temperature ranges of 800~1040 °C and strain rate ranges of 0.01~10 s⁻¹ is shown in Fig.14. For a constant strain, the DRX volume fraction increases with the decrease of strain rate and the increase of temperature. When the steel was deformed at higher temperature and lower strain rate, the grain boundary migration rate is accelerated and the occurrence of DRX is promoted. The calculated values correspond well with the experimental results, and the results indicate the accuracy of DRX volume fraction model.

2.5 Model for DRX grain size

According to the microstructure analysis in Section 2.3, it is found that the complete DRX grain size is mainly dependent on the strain rate and deformation temperature. The relationship between DRX grain size and deformation parameters can be described in terms of the power law function of Zener-Hollomon parameter Z and it is expressed as follows^[27]:

$$D = CZ^m \quad (10)$$

where C and m are experimental constants, D is complete DRX grain size. The values of C and m can be determined by the linear fitting of the plot of $\ln D - \ln Z$, as shown in Fig.15.

Based on the present experimental results, the constants C and m are calculated as 2.637×10^4 and 0.22, respectively. In summary, the model of DRX grain size of AerMet100 steel can be expressed as:

$$\begin{cases} D = 2.637 \times 10^4 Z^{-0.22} \\ Z = \dot{\varepsilon} \exp(396\,724/RT) \end{cases} \quad (11)$$

Fig.16 shows the comparison between the predicted and experimental results of the DRX grain size. It can be seen that the growth of DRX grains is properly sensitive to the deformation temperature and strain rate. The DRX grain size increases with the increase of temperature and the decrease of the strain rate, which is in agreement with microstructure analysis previously. And the results discussed above indicate

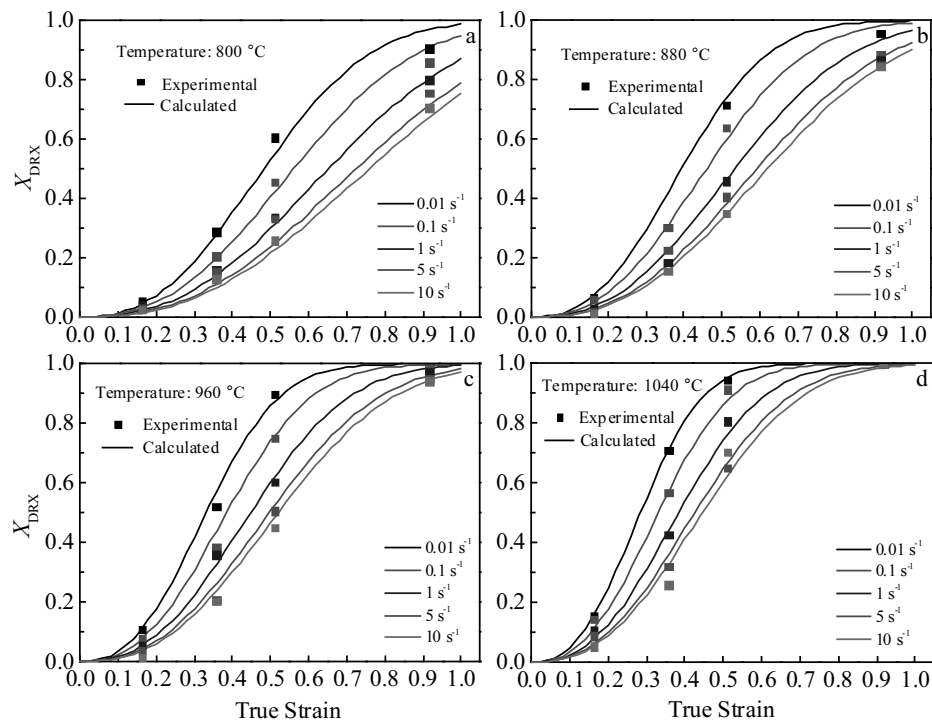


Fig.14 Comparison of the calculated and experimental DRX volume fraction: (a) 800 °C, (b) 880 °C, (c) 960 °C, and (d) 1040 °C

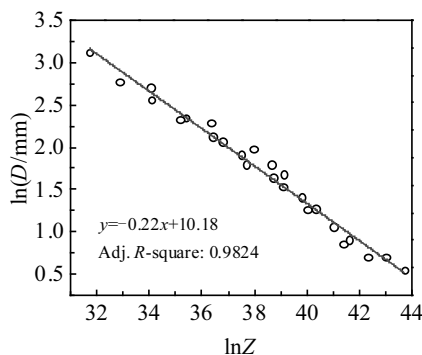


Fig.15 Plot of $\ln D$ vs $\ln Z$

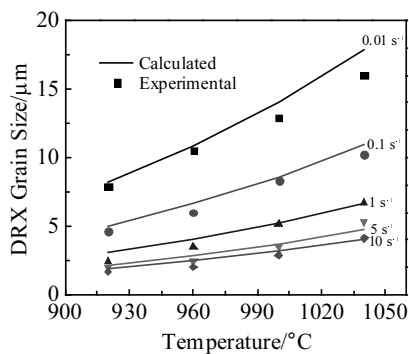


Fig.16 Comparison of the calculated and experimental DRX grain size

the high accuracy of the DRX grain size model for predicting the DRX behavior of AerMet100 steel.

3 Conclusions

1) The flow stresses of AerMet100 steel during thermo-mechanical processing can be greatly affected by the deformation parameters. The flow stress decreases with the increase of temperature and the decrease of strain rate.

2) The deformation activation energy of AerMet100 steel at the peak strain is calculated to be 396.724 kJ/mol. The relationship between flow stress and deformation parameters for Aermet100 steel can be determined by the Arrhenius constitutive equation:

$$\dot{\epsilon} = e^{37.07} [\sinh(5.18 \times 10^{-3} \sigma)]^{8.109} \exp(-396\,724/RT)$$

3) The kinetic models of DRX volume fraction (X_{DRX}) and grain size (D) are established by the analysis of flow curves and microstructures under different deformation conditions, and the correctness of this model is verified by microstructure.

References

- Li D, Gangloff R P, Scully J R. *Metallurgical and Materials Transactions A*[J], 2004, 35(3): 849
- Liu F C, Yu X B, Huang C P et al. *Journal of Wuhan University of Technology, Materials Science Edition*[J], 2015, 304(4): 827
- Ayer R, Machmeier P M. *Metallurgical Transactions A*[J], 1993, 24(9): 595
- Liu J, Li J, Cheng X et al. *Metallurgical and Materials*

- Transactions A*[J], 2017, 49: 595
- 5 Ji G, Li F, Li Q et al. *Materials Science & Engineering A*[J], 2010, 527(9): 2350
 - 6 Ji Guoqiang, Li Fuguo, Li Qinghua et al. *Computational Materials Science*[J], 2010, 48(3): 626
 - 7 Ji Guoqiang, Li Fuguo, Li Qinghua et al. *Materials Science & Engineering A*[J], 2011, 528: 4774
 - 8 Hu D Y, Meng K P, Jiang H L et al. *Materials & Design*[J], 2015, 87: 759
 - 9 Hu D Y, Meng K P, Jiang H L et al. *Procedia Engineering*[J], 2015, 99: 1459
 - 10 Poliak E I, Jonas J I. *Acta Materialia*[J], 1996, 44(1): 127
 - 11 Ning Y Q, Wang T, Fu M W et al. *Materials Science & Engineering A*[J], 2015, 642: 187
 - 12 Tan K, Li J, Guan Z J et al. *Materials & Design*[J], 2015, 84: 204
 - 13 Imbert C A C, McQueen H J. *Materials Science & Engineering A*[J], 2001, 313(1-2): 104
 - 14 Liang H Q, Nan Y, Ning Y Q et al. *Journal of Alloys and Compounds*[J], 2015, 632: 478
 - 15 Chen X M, Lin Y C, Chen M S et al. *Materials & Design*[J], 2015, 77: 41
 - 16 Chen M S, Lin Y C, Ma X S. *Materials Science & Engineering A*[J], 2012, 55: 260
 - 17 Sellars C M, McTegart W J. *Acta Metallurgica*[J], 1966, 14(9): 1136
 - 18 Zener C, Hollomon J H. *Journal of Applied Physics*[J], 1944, 15(1): 22
 - 19 Takuda H, Fujimoto H, Hatta N. *Journal of Materials Processing Technology*[J], 1998, 80: 513
 - 20 Quan G Z, Luo G C, Liang J T et al. *Computational Materials Science*[J], 2015, 97: 136
 - 21 Sakai T, Belyakov A, Kaibyshev R et al. *Progress in Materials Science*[J], 2014, 60(1): 130
 - 22 Dehghan M A, Barnett M R, Hodgson P D. *Metallurgical and Materials Transactions A*[J], 2008, 39(6): 1359
 - 23 Kang J Y, Kim H, Son D et al. *Materials Characterization*[J], 2018, 135: 8
 - 24 Sellars C M. *Materials Science and Technology*[J], 1990, 6(11): 1072
 - 25 Wang K L, Fu M W, Lu S Q et al. *Materials & Design*[J], 2011, 32(3): 1283
 - 26 Lin Y C, Chen M S, Zhong J. *Materials & Design*[J], 2009, 30(3): 908
 - 27 Sellars C M, Whiteman J A. *Metal Science*[J], 1979, 13(3-4): 187

AerMet100 超高强度钢在热加工过程中的动态再结晶模型

赵张龙, 闵晓楠, 徐文馨, 曹澜川, 张 鸽, 宋旭阳, 李 晖

(西北工业大学, 陕西 西安 710072)

摘 要: 为了准确预测 AerMet100 超高强度钢在热加工过程中的微观组织演变, 通过一系列等温热压缩试验, 建立了包括动态再结晶 (DRX) 体积分数和 DRX 晶粒尺寸在内的 DRX 模型。分析了该合金在温度范围为 800~1040 °C 和应变速率范围为 0.01~10 s⁻¹ 的条件下变形 15%~60% 的热变形行为。通过计算获得了 AerMet100 钢本构模型中的 Zener-Hollomon 参数, 建立了 DRX 模型。通过建立的 DRX 模型定量预测了热变形参数对该合金微观组织演变的影响。进一步观察微观组织发现, 高温低应变速率和较大的变形程度有利于 DRX 的充分发生, 使组织细化和均匀化。模型预测结果与实验结果吻合较好, 验证了所建立的 DRX 模型的准确性。结果表明, DRX 模型可以定量预测 AerMet100 钢构件在不同变形条件下进行热力学加工时的微观组织演变规律。

关键词: AerMet100 钢; 动态再结晶; 热变形; 显微组织

作者简介: 赵张龙, 男, 1981 年生, 博士, 副教授, 西北工业大学材料科学与工程学院, 陕西 西安 710072, 电话: 029-88492642, E-mail: zlzhaol@nwpu.edu.cn